Shear Stress Regulates ABCA1-dependent Membrane Cholesterol Content in Endothelial Cells Facilitating H_2S-dependent Vasodilation

Jacob R. Anderson, Nancy L. Kanagy, Laura V. Gonzalez Bosc, Jay S. Naik*

*Corresponding author: jnaik@salud.unm.edu

University of New Mexico Health Science Center
MSC08 4750
Department of Cell Biology and Physiology
Albuquerque, NM 87131

Running Head: ABCA1 and membrane cholesterol

Key Words: shear stress, mesenteric, vasodilation, hydrogen sulfide, Sprague-Dawley rat

Jacob R. Anderson[1], Laura V. Gonzalez Bosc[1], Nancy L. Kanagy[1], and Jay S. Naik[1]

[1]Vascular Physiology Group, Department of Cell Biology and Physiology, University of New Mexico Health Sciences Center, Albuquerque, NM, USA

Abstract:

Endothelial cells (ECs) express an array of integral membrane proteins, including ion channels and transporters that contribute to blood flow regulation and cell-cell communication. Many of these membrane proteins are regulated by plasma membrane cholesterol content. The ATP-binding cassette family a1 (ABCA1) transporter is a regulator of membrane cholesterol content. We have shown increased ABCA1 mRNA expression and reduced EC membrane cholesterol in resistance mesenteric arteries compared to conduit arteries. Previous studies suggest shear stress (SS) can increase or decrease ABCA1 expression in a cell-type-dependent manner. *Hypothesis*: SS sustains lower EC membrane cholesterol concentration through ABCA1-mediated cholesterol transport, facilitating H_2S-mediated vasodilation. *Method*s: The effect of SS on ABCA1 and membrane cholesterol content was assessed in pressurized mesenteric arteries from male Sprague-Dawley rats and cultured human aortic endothelial cells. Pressure myography was used to assess the effects of ABCA1 inhibition on H_2S-mediated vasodilation. Filipin was used to assess EC membrane cholesterol content. *Results*: SS increased ABCA1 expression in the endothelium of mesenteric arteries and cultured human aortic endothelial cells and markedly reduced EC membrane cholesterol. Inhibition of ABCA1 increased EC membrane cholesterol content and abolished H_2S-induced vasodilation. *Conclusion:* SS facilitation of EC-dependent vasodilation appears to be mediated by membrane cholesterol content.

58 **Introduction:**

59 The endothelium comprises a monolayer of highly specialized endothelial cells
60 (ECs) lining the luminal surface of all blood vessels and occupies a fundamental position
61 in the cardiovascular system. The endothelium regulates complex intercellular
62 interactions, including vascular tone, vascular permeability, and innate immune
63 response[1,2]. The endothelium senses and integrates various stimuli to regulate vascular
64 tone through the synthesis and release of vasoactive gas molecules, such as nitric oxide,
65 carbon monoxide, and hydrogen sulfide (H_2S) [3].

66 H_2S has been reported to be an endothelial-derived hyperpolarization factor
67 contributing to vasodilation[4] and exerting antioxidant and anti-inflammatory protective
68 effects on the cardiovascular system[5]. The enzymatic synthesis of H_2S involves
69 cystathionine-γ-lyase, cystathionine-β-synthase, and 3-mercaptopyruvate
70 sulfurtransferase; the specific enzymatic pathways vary across vascular beds, adding
71 complexity to the regulation of H_2S-mediated vasodilation[6,7]. Our previous work has
72 shown that H_2S sensitivity in conduit arteries (>300 μm) is dependent on the content of
73 membrane cholesterol in ECs, whereas resistance arteries (<150 μm) are inherently
74 sensitive to H_2S[8].

75 Membrane cholesterol is a fundamental constituent of the lipid bilayer, impacting
76 membrane fluidity, stability, and organization[9]. Interestingly, our lab has shown that native
77 EC membrane cholesterol content is greater in EC from conduit arteries than in those
78 from resistance arteries,[8] suggesting innate regional differences in membrane cholesterol
79 content along the vascular tree. In addition, our single-cell RNAseq analysis supported
80 by immunohistochemistry indicates that ECs from resistance arteries express greater

levels of the reverse cholesterol transport genes ATP-binding cassette protein A1 (ABCA1) and phospholipid transfer protein (PLTP) compared to ECs from conduit vessels[10]. The ATP-binding cassette (ABC) transport proteins, a family of eight genes, are responsible for transporting various hydrophobic compounds across membranes. ABCA1 specifically facilitates membrane cholesterol efflux through a process called reverse cholesterol transport in multiple cell types[11,12]. Taken together, these findings suggest that reduced membrane cholesterol within resistance arteries enhances endothelial-mediated vasodilation, supporting the postulate that membrane cholesterol is an important mediator of EC function. However, despite the observed regional heterogeneity in ABCA1 expression within the vascular tree, it is unknown whether ABCA1 mediates innate differences in EC cholesterol content. Additionally, the mechanism mediating the differential ABCA1 expression between conduit and resistance arteries also remains unknown. Previous studies suggest shear stress (SS) can both increase and decrease ABCA1 expression, potentially in a cell-type-dependent manner[13–15].

Vascular SS is a mechanical force resulting from friction against the endothelium generated by blood flowing along its surface. Vascular ECs sense SS through the activation of mechanosensors, translating it into biochemical signals influencing cell morphology, vascular tone, and gene expression[16,17]. As the luminal diameter of an artery decreases, SS exponentially increases[18], suggesting that differences in SS may mediate cellular heterogeneity along the vascular tree. Therefore, we hypothesized that SS sustains lower EC membrane cholesterol concentration through ABCA1-mediated cholesterol transport, facilitating H_2S-mediated vasodilation.

104 **Methods**

105 Cell Culture

106 Primary HAoECs (Cell Applications S304-05a, P4-P6) were used for all cell culture
107 experiments. Cells were plated on cell culture dishes coated with 0.1% Fibronectin
108 (Sigma, FC010) and maintained at 37°C, 5% CO_2 in endothelial growth media V2 (Cell
109 Applications). To expose cells to SS, ECs were seeded on μ-Slide 0.4 Luer ibiTreat (ibidi
110 80176). Unidirectional, recirculating, laminar flow was applied to confluent monolayers
111 using a peristaltic pump [6 dyne/cm^2, 20 dyne/cm^2, or 0 dyne/cm^2 for static control] with
112 an inline wind Kessel (to dampen pulsatile oscillations) and bubble trap.

113

114 Animals

115 Sprague-Dawley rats (Envigo, 250–300 g, 9–10 wk. old) were used for all
116 experiments. Rats were euthanized with a lethal concentration of pentobarbital sodium
117 (200 mg/kg I.P.), and mesenteric arteries were collected for experiments. The Institutional
118 Animal Care and Use Committee of the University of New Mexico School of Medicine
119 reviewed and approved all animal protocols. All protocols conformed to National Institutes
120 of Health guidelines for animal use.

121 Preparation of Endothelial Tubes

122 The mesenteric arcade was removed and immediately placed in ice-cold HEPES buffered
123 physiological saline solution (HPSS; in mM: 130 NaCl, 4 KCl, 1.2 $MgSO_4$, 4 $NaHCO_3$, 1.8
124 $CaCl_2$, 10 HEPES, 1.18 KH_2PO_4, and 6 glucose; pH adjusted to 7.4 with NaOH),

125 containing 10 μM sodium nitroprusside and 0.1% bovine serum albumin (BSA). Veins
126 were removed, and arteries were cleared of connective and adipose tissue. Arteries (50-
127 150μm) were flushed of blood and pretreated with probucol (100 μM in 2% pluronic acid)
128 or vehicle at 37°C for 1 hour in HPSS containing 10% FBS and 0.1% bovine serum
129 albumin. Endothelial tubes were isolated as previously described[19]. Briefly, arteries were
130 then placed in an HPSS digestion solution (10% FBS, 0.1% bovine serum albumin, 0.62
131 mg/mL of papain, 1.5 mg/ mL of collagenase II, and 1 mg/mL dithiothreitol) with continued
132 treatment with probucol or vehicle. The arteries were incubated in the digestion solution
133 for 33 minutes at 37°C. The digestion solution was replaced with ice-cold HEPES buffered
134 physiological saline solution (HPSS; in mM: 130 NaCl, 4 KCl, 1.2 $MgSO_4$, 4 $NaHCO_3$, 1.8
135 $CaCl_2$, 10 HEPES, 1.18 KH_2PO_4, and 6 glucose; pH adjusted to 7.4 with NaOH), 10%
136 FBS and 0.1% BSA and artery segments were gently triturated to disrupt the adventitia
137 and smooth muscle layers. Isolated EC tubes are then transferred using a transfer pipette
138 and allowed to adhere to a glass slide. A pap-pen was used to create a hydrophobic
139 pocket on the slide with sufficient surface tension to hold the EC tubes, antibody, and
140 other solutions within a confined area. A Hamilton 250μL glass syringe was used to apply
141 staining solutions and perform washes. EC tubes were mounted with ProLong Gold
142 antifade mounting reagent.

143 Quantification of Membrane Cholesterol Content

144 Isolated endothelial tubes were plated on glass coverslips and fixed with 4%
145 paraformaldehyde (20 min at RT). Endothelial cell membrane cholesterol was detected
146 by incubating cells with the fluorescent cholesterol marker filipin III (100 μg/mL) for 45
147 minutes at 37 °C under light-protected conditions. Coverslips were then mounted on

148 slides using Prolong Gold Antifade (Thermo Fisher P10144). Samples were imaged using
149 a fluorescent confocal microscope (Zeiss LSM 800 AxioObserver.Z1/7; Gottingen,
150 Germany) with a 353 nm laser (excitation) and a 465 nm long-pass filter (emission),
151 combined with a Plan-Apochromat 63/1.4 numerical aperture (NA) oil immersion
152 objective. A negative control lacking filipin was used to control for background signal.
153 Filipin staining was quantified using ImageJ[20]. A total of 4 tubes/artery from five animals
154 were analyzed. The mean fluorescence intensity of each endothelial tube was measured
155 and averaged to determine a mean fluorescence value for each animal.

156 HAoECs were stained as previously described above with filipin, and the samples
157 were imaged using a Zeiss LSM800. Images contained 8-10 images with 7-10 cells per
158 image for three independent experiments. Regions of interest were created at
159 approximately 1 mm from the membrane, both intra- and extracellularly, to isolate the
160 membrane from the intracellular compartments. Images were collected within one optical
161 section showing membrane max diameter to ensure the focus was on the cell center, and
162 the mean fluorescence intensity per cell was measured and averaged to determine
163 cholesterol content.

164 Quantification of ABCA1 Protein Expression

165 Endothelial ABCA1 expression was quantified using immunofluorescence in *en-*
166 *face* small arteries and HAoECs. Small (<150 μm) were cannulated and pressurized[21].
167 Briefly, pressurized mesenteric arteries were fixed with 4% paraformaldehyde for 20
168 minutes at room temperature. Samples were blocked with 5% non-donkey serum (NDS)
169 and treated with ABCA1 primary antibody (1:100) (Thermo Fisher, PA1-16789) overnight
170 at 4ºC. Endothelial tubes were then blocked with 5% NDS for 1 h at 37ºC and incubated

171 with donkey-α-rabbit 488 (1:1000) (Jackson ImmunoResearch Labs, 711-546-152) in 1%
172 NDS for 4 h at 37ºC. Samples were mounted with Prolong Gold Antifade DAPI (Thermo
173 Fisher, P36935), and z-stack images were acquired using confocal microscopy (Zeiss
174 LSM 800 AxioObserver.Z1/7) using a 488 nm laser (excitation) and 517 nm long pass
175 filter (emission) and a Plan-Apochromat 63/1.4 NA oil immersion objective. Secondary
176 antibody controls were used to verify the lack of non-specific staining. A total of 4
177 tubes/animal from five animals were analyzed. Z-stacks containing 14-16 slices each at
178 150nm were obtained, maximum projections were generated, and the mean fluorescence
179 intensity (MFI) of each endothelial tube was measured using ImageJ and averaged to
180 determine a mean fluorescence value for each animal.

181 For the HAoECs, ECs were exposed to shear stress (6 dynes/cm^2 or 20 dyne/cm^2)
182 or static conditions for 24 hours using a parallel flow chamber prior to fixation with 4%
183 PFA. HAoECs were blocked with 5% NDS and treated with ABCA1 primary antibody
184 (1:100) (Thermo Fisher, PA1-16789) or CSE (1:100 Proteintech, 12217-1-AP) overnight
185 at 4 ºC. HAoECs were then blocked with 5% NDS for 1 hour at 37 ºC and incubated with
186 donkey-α-rabbit 488 (1:1000) in 1% NDS for 4 hours at 37 ºC. Samples were mounted
187 with Prolong Gold Antifade DAPI. Images contained 8-10 images with 7-10 cells per
188 image for three independent runs, and the MFI was determined using ImageJ. The LXR
189 agonist T0901317 (100 nM) is a well-established inducer of ABCA1 expression and was
190 used to validate the specificity of the ABCA1 antibody (Fig. 6).

191 Application of SS to Mesenteric Arteries

192 Mesenteric conduit arteries (>300 μm) were cannulated and pressurized to
193 65mmHg using a gravity-based column system. Luminal flow was generated by adjusting

194 the column heights [$P_{arterial}$ ~130mmHg and P_{venous} ~35mmHg (HSS)]. Arteries were
195 continuously superfused with HPSS (5 ml/min, 37°C). Mean pressure was maintained at
196 65 mmHg. Vessels were exposed to flow for 6 hours, followed by a viability response
197 (Ach-dilation), before fixation with 4% PFA for 20 minutes while being continually
198 pressurized. Vessels were then cut along their longitudinal axis, secured *en face,* and
199 blocked with 5% NDS for 1 hour at room temperature. Vessel segments were then
200 incubated overnight at 4 °C with ABCA1 primary antibody (1:100 – PA1-16789, Thermo)
201 in 1% NDS in phosphate-buffered saline. Secondary antibody AF-488 (1:1000, Jackson
202 Lab) was applied for 1 hour at room temperature in 1% NDS in phosphate-buffered saline
203 and mounted with Prolong Gold. Five images from various parts of the artery were
204 captured per condition. ABCA1 intensity was measured using ImageJ.

205

206 RT-qPCR Studies

207 HAoECs were exposed to either static, 6 dynes/cm², or 20 dynes/cm² conditions
208 for 24 hours. In a separate set of experiments, HAoECs were treated with methyl-β-
209 cyclodextrin (MβCD, 1mM) to deplete membrane cholesterol or MβCD + cholesterol
210 (MβCD-Chol, 20mM) to increase membrane cholesterol content for 24 hours. RNA was
211 isolated using an RNA extraction kit (Macherey-Nagel, 740955.50) according to the
212 manufacture's recommendations. cDNA was generated with 0.1 µg of RNA using the
213 High-Capacity cDNA Reverse Transcription Kit (Thermo, 4374967). qPCR was performed
214 using the TaqMan Fast Advanced Master Mix (Thermo 4444556). TaqMan Gene
215 Expression Assay Primers for ABCA1 (4331182) and GAPDH (4331182) were purchased

216 from Thermofisher. GAPDH was used as a housekeeping gene to normalize the
217 expression of ABCA1. Data was normalized using the 2-delta CT method.

218 Vasodilation Studies

219 The mesenteric arcade was removed and immediately placed in ice-cold HPSS.
220 After the removal of veins and adipose tissue, third- to fourth-order mesenteric arteries
221 (with an inner diameter of 100–200 μm) were isolated and cannulated with glass
222 micropipettes, and gently flushed to remove blood from the lumen, as previously
223 described[22,23]. The artery was stretched longitudinally to approximate its in situ length and
224 pressurized with a servo-controlled peristaltic pump (Living Systems) to 75 mmHg. The
225 vessel chamber was superfused with HPSS at 5 ml/min at 37°C and allowed to equilibrate
226 for 15 min. To determine the contribution of ABCA1 on the H_2S-mediated vasodilatory
227 response, arteries were pretreated luminally with the specific ABCA1 antagonist, probucol
228 (100 μM), for one hour before arteries were pre-constricted to ~30–50% with the
229 thromboxane A_2 analog, U-46619 (Cayman Chemical). To assess H_2S-mediated
230 vasodilation, arteries were treated with sodium hydrosulfide (NaHS) at concentrations of
231 1, 10, and 30 μM (Cayman Chemical). Images were obtained using an Eclipse TS100
232 microscope (Nikon) and CCD100M camera to measure ID using edge-detection software
233 (IonOptix). Passive diameter was determined at the end of each experiment by
234 superfusing the vessel in Ca^{2+}-free HPSS HPSS containing: 130 NaCl, 4 KCl, 1.2 $MgSO_4$,
235 3.6 EGTA, $NaHCO_3$, 10 HEPES, 1.18 KH_2PO_4, and 6 glucose; pH adjusted to 7.4 with
236 NaOH), containing 10 μM sodium nitroprusside and 0.1% bovine serum albumin (in mM)
237 for 30 min. For all experiments, changes in vessel diameter (plateau response) are
238 expressed as the percent reversal of U46619-induced vasoconstriction.

239 Cholesterol efflux

240 HAoECs were cultured in the presence of probucol (100 μM) or vehicle for
241 24 hours. The media was then used to assess cholesterol efflux using Amplex-Red,
242 according to the manufacturer's instructions (Thermo Fisher A12216). A subset of
243 experiments were also exposed to static or HSS conditions for 24 hrs.

244 Statistics and Calculations

245 All data are expressed as means ± SD. Statistical comparisons were made using
246 Prism 9 (GraphPad Software). The specific statistical tests used are reported in the figure
247 legends. A probability of <0.05 was accepted as statistically significant for all
248 comparisons. Percent dilation was calculated as (NaHS diameter – U46619 diameter) /
249 (Calcium Free diameter – U46619 diameter) x100%.

250

251 **Results**

252 **Effect of SS on ABCA1 expression and membrane cholesterol in HAoECs**

253 We exposed HAoECs to a SS of 6 dynes/cm^2, 20 dynes/cm^2, or static conditions
254 for 24 hrs. Application of SS increased protein ABCA1 expression in HAoEC (Fig. 1a,b).
255 SS reduced Abca1 mRNA levels in HAoEC (Fig. 1c). Depletion of membrane cholesterol
256 reduced ABCA1 mRNA levels. Conversely, supplementing membrane cholesterol
257 increased ABCA1 mRNA levels (Fig. 1d). To validate that changes in ABCA1 were
258 associated with reductions in membrane cholesterol, we employed filipin staining to

259 demonstrate that exposing cells to SS reduces the cholesterol content of the EC
260 membrane (Fig. 2).

261

262 **Effect of SS on ABCA1 expression in mesenteric conduit arteries**

263 To assess the effect of SS on ABCA1 expression, pressurized mesenteric arteries were
264 exposed to either 12 or 20 dynes/cm^2 for 6 hours before fixation. SS elicited an increase
265 in ABCA1 expression compared to arteries exposed to 12 dyn/cm^2 SS (Fig.3). We have
266 previously examined ABCA1 expression in freshly isolated paraformaldehyde-fixed
267 endothelial cell tubes from both large and small mesenteric arteries.[24] ABCA1 expression
268 and membrane cholesterol were significantly lower in tubes from large arteries compared
269 to small resistance arteries. ABCA1 expression appears greater in freshly isolated EC
270 compared to arteries exposed to SS ex vivo. The difference in expression between the
271 freshly isolated EC and arteries exposed to 6 hours of ex vivo flow may be due to
272 differences in the absolute magnitude of shear stress in the two settings.

273

274 **Effect of ABCA1 inhibition on membrane cholesterol and H_2S-mediated**
275 **vasodilation in mesenteric resistance arteries**

276 Inhibition of EC ABCA1 in small mesenteric arteries (<150 μm) increased EC
277 membrane cholesterol and reduced cholesterol efflux from HAoECs (Fig. 4a-c). In
278 addition, inhibition of ABCA1 significantly attenuated the SS-induced increase in
279 cholesterol efflux (Fig 4d). Administration of increasing concentrations of H_2S elicited a

280 dose-dependent vasodilation in arteries treated with the vehicle. Inhibition of ABCA1
281 attenuated H_2S-mediated vasodilation compared to control (Fig. 5).

282

283 **Discussion**

284 Endothelial function is crucial for maintaining vascular homeostasis, and
285 disruptions in endothelial signaling pathways can lead to the development of
286 cardiovascular disease. This study demonstrates a novel role for ABCA1 in regulating
287 membrane cholesterol levels in endothelial cells. To our knowledge, this is the first study
288 to demonstrate a role for ABCA1 in SS-mediated reductions in membrane cholesterol.
289 The findings suggest that ABCA1 regulation of membrane cholesterol impacts hydrogen
290 sulfide (H_2S)-mediated vasodilation with potential implications for the regulation of
291 microvascular function and disease pathophysiology. The key findings of this study are
292 (1) SS increased ABCA1 expression in endothelial cells but reduced mRNA transcripts,
293 (2) inhibition of ABCA1 increased membrane cholesterol levels and reduced cholesterol
294 efflux, and (3) ABCA1 inhibition attenuated H_2S-mediated vasodilation.

295 The regulation of membrane cholesterol by ABCA1 in resistance arteries has
296 significant physiological implications. Resistance-sized arteries are critical regulators of
297 vascular resistance and blood pressure, and their endothelial function is highly influenced
298 by membrane cholesterol content[25,26]. Our previous work demonstrated that five up-
299 regulated, differentially expressed genes involved in cholesterol transport
300 (Nfkbia, Apoe, Lrp1, Abca1, Pltp) were present in ECs from small mesenteric arteries
301 compared to ECs from large arteries. NF-kappa-B inhibitor alpha (*NFKBIA*) has been

302 shown to enhance cholesterol transport in macrophages by inhibiting NFKB,[27,28], whereas
303 ApoE facilitates cholesterol transport through direct binding with ABCA1[29,30]. The low-
304 density lipoprotein receptor-related protein (*LRP1*) has been shown to regulate lipid and
305 glucose metabolism and is a known co-activator of a transcriptional regulator of ABCA1,
306 PPAR gamma[31,32,33]. Moreover, phospholipid transfer protein (*PLTP*) functions as an
307 auxiliary protein that facilitates ABCA1-mediated cholesterol transport[34]. This gene
308 ontology pathway analysis related to cholesterol transport supports the postulate that
309 ABCA1 is a key determinant of membrane cholesterol heterogeneity.

310 Our previous work has shown that H_2S-mediated vasodilation in rat mesenteric
311 arteries involves the activation of EC transient receptor potential cation subfamily V
312 member 4 channel (TRPV4) channels and EC large conductance (BK_{Ca}) Ca^{2+}-activated
313 potassium channels (Morin et al. 2022). TRPV4 and BK_{ca} contain cholesterol
314 recognition/interaction amino acid consensus sequences (CRAC/CARC)[35,36]. Indeed,
315 membrane cholesterol has been shown to negatively regulate TRPV4 and BK_{Ca} channel
316 activity through direct protein-sterol interactions[35,37]. In addition to channel regulation via
317 direct protein-sterol interactions, changes in membrane cholesterol may alter signaling
318 microdomains. We have previously demonstrated that the depletion of membrane
319 cholesterol is required to demonstrate a role for TPRV4 channels in muscarinic receptor-
320 mediated vasodilation in rat gracilis arteries (Morin et al., 2022). In addition, we have
321 demonstrated that depletion of membrane cholesterol with MbCD in arteries with higher
322 cholesterol content (large mesenteric arteries) enhances H_2S dilation. Conversely,
323 loading arteries with MBCD-chol in arteries with lower native cholesterol content (small
324 arteries) abolished H_2S-mediated vasodilation. Interestingly, loading these arteries with

325 the cholesterol enantiomer, epicholesterol, did not affect H_2S vasodilation in these
326 arteries. Suggesting that the effect of cholesterol on H_2S vasodilation is due to protein-
327 sterol interactions rather than changes in physical properties of the membrane (e.g.,
328 membrane fluidity).[38] Our current findings suggest that increases in membrane
329 cholesterol through ABCA1 inhibition attenuates H_2S-mediated vasodilation in rat
330 mesenteric resistance arteries, and cholesterol efflux was reduced in HAoECs. Our
331 findings suggest that ABCA1 regulates endothelial membrane cholesterol by reducing
332 cholesterol and potentiating the dilatory effect of H_2S.

333 SS has been recognized as a key determinant of endothelial phenotype influencing
334 processes such as nitric oxide production[39], cellular polarization[40], inflammation[41,42], and
335 permeability[43]. A previous report demonstrated a potential mechanism for enhanced
336 ABCA1 expression in response to SS. Zhu *et al.* observed increases in key transcription
337 factors involved in lipid homeostasis and ABCA1 regulation in human umbilical vein
338 endothelial cells exposed to 2 dynes/cm^2 or 12 dynes/cm^2 SS. In addition, their findings
339 suggest that SS increases mRNA levels of the CYP27A gene, which is responsible for
340 oxysterol production. Additionally, mRNA levels of LXRα, an oxysterol-activated
341 transcriptional regulator of *Abca1,* were increased in response to SS[13]. In contrast, Li *et*
342 *al.* demonstrated that SS (40 dynes/cm^2) reduced ABCA1 expression in human brain
343 endothelial cells[14]. These discrepancies may be due to cell type differences or the
344 magnitude of the applied shear stress. Our data suggest that increases in SS increase
345 the expression of ABCA1, indicating that cholesterol transport mechanisms are actively
346 modulated in response to shear stress. We demonstrated that HAoECs exposed to SS
347 exhibit reduced membrane cholesterol levels compared to cells under static conditions.

348 In addition, this decrease in plasma membrane cholesterol was associated with a shift in
349 the localization of free cholesterol to an endosomal-like state and ABCA1 has been shown
350 to reside on the cell surface as well as endosomal compartments[44]. Notably, the
351 application of shear stress reduced ABCA1 mRNA transcript levels despite a significant
352 increase in ABCA1 protein. The sterol regulatory element-binding protein2 (SREBP2) is
353 a critical regulator of genes involved in cellular cholesterol homeostasis. Classically, a
354 decrease in cellular cholesterol leads to the activation and translocation of SREBP2 to
355 the nucleus, thereby promoting the expression of genes involved in cholesterol uptake
356 and de novo synthesis and suppressing the expression of cholesterol efflux genes[45]. In
357 the present study, we observed that SS increased ABCA1 protein expression, which is
358 associated with decreased membrane cholesterol and Abca1 mRNA levels. In addition,
359 we demonstrate that depletion of membrane cholesterol with MbCD decreased Abca1
360 mRNA. In contrast, cholesterol supplementation increased Abca1 mRNA levels (Fig. 1).
361 Taken together, these results suggest that SS may stabilize ABCA1, promoting
362 cholesterol efflux, and that the loss of membrane cholesterol results in a downregulates
363 Abca1 mRNA. One consideration in our cell culture model could be a change in the
364 degradation rate, such that higher flow rates may protect ABCA1 from calpain-mediated
365 degradation. Several studies have demonstrated the transcriptional and translation
366 regulation of ABCA1 in the presence of cholesterol-depleting agents such as MBCD or
367 Apo-A1. Studies suggest activation of ABCA1 to flux cholesterol from the cell resulted in
368 stabilization of the ABCA1 complex and reduction in transcripts. Arakawa et al.
369 demonstrate that apoA-1 binding to ABCA1 during cholesterol efflux protects the protein
370 from degradation, increasing protein levels, which is associated with a decrease in

371 ABCA1 transcript levels[46]. Over time, in response to continuous SS, a new set point for
372 cholesterol homeostasis would be established, balancing cholesterol efflux, uptake, and
373 synthesis[47].

374 This study provides evidence that ABCA1 mediates cholesterol transport and
375 regulates membrane cholesterol levels in endothelial cells, and that reductions in
376 membrane cholesterol content facilitate ion channel activity, contributing to H_2S signaling
377 and promoting vasodilation. Taken together, these findings provide compelling evidence
378 for a novel role for ABCA1 in vascular endothelial function. Our data also show that
379 ABCA1 is a key mediator of endothelial membrane cholesterol in endothelial cells and
380 that shear stress influences the expression of ABCA1, thereby regulating membrane
381 cholesterol levels.

382 Funding sources

383 This research was supported by NIH Grants R01 HL160606-01 (J.S.N.), 5T32HL007736-
384 25 (J.R.A.), the University of New Mexico (UNM), UNM Comprehensive Cancer Center
385 Support Grant NCI P30CA118100, the Fluorescence Microscopy Shared Resource
386 Facility.

387 Disclosures

388 No conflicts of interest, financial or otherwise, are declared by the authors.

389 Author contributions

390 J.R.A., L.V.G.B., N.L.K., and J.S.N. conceived and designed research; J.R.A. performed
391 experiments; J.R.A. analyzed data; J.R.A., L.V.G.B., N.L.K., and J.S.N. interpreted results

392 of experiments; J.R.A. and J.S.N. prepared figures; J.R.A. drafted manuscript; J.R.A.,
393 L.V.G.B., N.L.K., and J.S.N. edited and revised manuscript; J.R.A., L.V.G.B., N.L.K., and
394 J.S.N. approved final version of manuscript.

395

396 Figure 1. Shear stress increases ABCA1 expression. (A) Representative images of
397 ABCA1 expression (yellow) in response to static, 6 dynes/cm^2, or 20 dynes/cm^2 in human
398 aortic endothelial cells. (B) Quantification of mean fluorescence intensity for ABCA1
399 expression. 8-10 images were acquired per condition (n=5/group) with 6 – 7 cells per
400 image. (C) ABCA1 mRNA expression normalized to GAPDH in response to static
401 conditions, 6 dynes/cm^2, or 20 dynes/cm^2 in HAoECs. (D) ABCA mRNA in response to
402 cholesterol manipulation in HAoECs. One-way ANOVA with Tukey's Post-hoc test was
403 used for statistical analysis.

404 Figure 2. Shear stress decreases membrane cholesterol. (A) Representative images of
405 membrane cholesterol expression in response to static, 6 dynes/cm^2, or 20 dynes/cm^2 in
406 human aortic endothelial cells. (B) Quantification of mean fluorescence intensity for filipin
407 III staining (orange) for the plasma membrane and (C) internal cholesterol content. 8-10
408 images per condition (n=3/group) with 6 – 7 cells per image were acquired. One-way
409 ANOVA with Tukey's Post-hoc test was used for statistical analysis.

410 Figure 3. Increasing shear stress increases ABCA1 expression. (A) Representative
411 images of ABCA1 expression in response to increasing shear stress in intact large
412 mesenteric arteries. (B) Quantification of mean fluorescence intensity expressed as fold
413 change for ABCA1 expression. Five images per artery were acquired per condition

414 (n=3/group). Nuclear stain DAPI (magenta), ABCA1 (green). Student's t-test was used for
415 statistical analysis.

416 Figure 4. Inhibition of ABCA1 increases membrane cholesterol and reduces cholesterol
417 efflux. (A) Representative images of membrane cholesterol in response to vehicle or
418 probucol in endothelial tubes isolated from small mesenteric arteries (< 150 μm). (B)
419 Quantification of mean fluorescence intensity for filipin III staining (yellow). 4 tubes/artery
420 from 5 animals. (C) Quantification of cholesterol efflux from HAoECs. One-way Anova
421 was used for statistical analysis. (D) Quantification of cholesterol efflux from HAoECs in
422 response to shear stress. Student's t-test or One-Way ANOVA with Tukey's Post-hoc test
423 was used for statistical analysis. **** P<0.0001, *** P< 0.0007.

424 Figure 5. Inhibition of ABCA1 attenuates H_2S-mediated vasodilation. (A) Representative
425 trace of vehicle treated artery, The red arrow indicates pre-constrictor U46619, black
426 arrows indicate H_2S dosage, and the blue arrow indicates Ca^{2+} free PSS. (B)
427 representative trace of probucol treated artery. (C) Summary responses of NaHS-
428 dependent dilation in arteries treated with vehicle (n = 5) or the ABCa1 inhibitor probucol
429 (100 μM, n = 5). Unpaired students t test was used for statistical analysis.

430 Figure 6. The liver X receptor agonist (T0901317) increases ABCA1 expression in
431 HAoECs. (A) Representative images of ABCA1 expression in response to vehicle
432 (DMSO) or T09 (10 μM and 100 μM). (B) Quantification of mean fluorescence intensity
433 for ABCA1 expression. 8-10 images per condition (n=3) with 6 – 7 cells per image. One-
434 way ANOVA with Tukey's Post-hoc test was used for statistical analysis.

435

436

437 Fig 1.

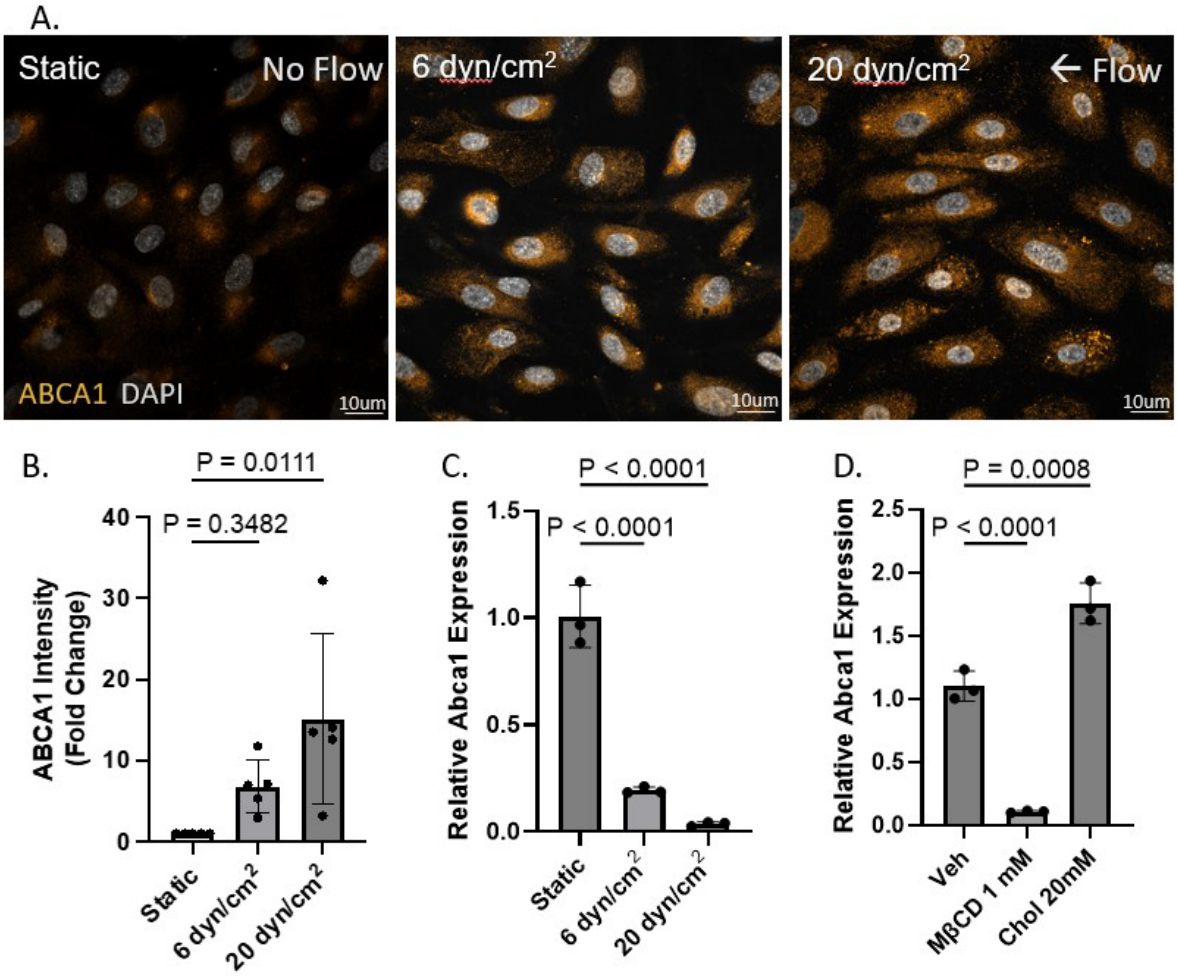

438

439

440

441

442

443

444

445

446

447 Fig 2.

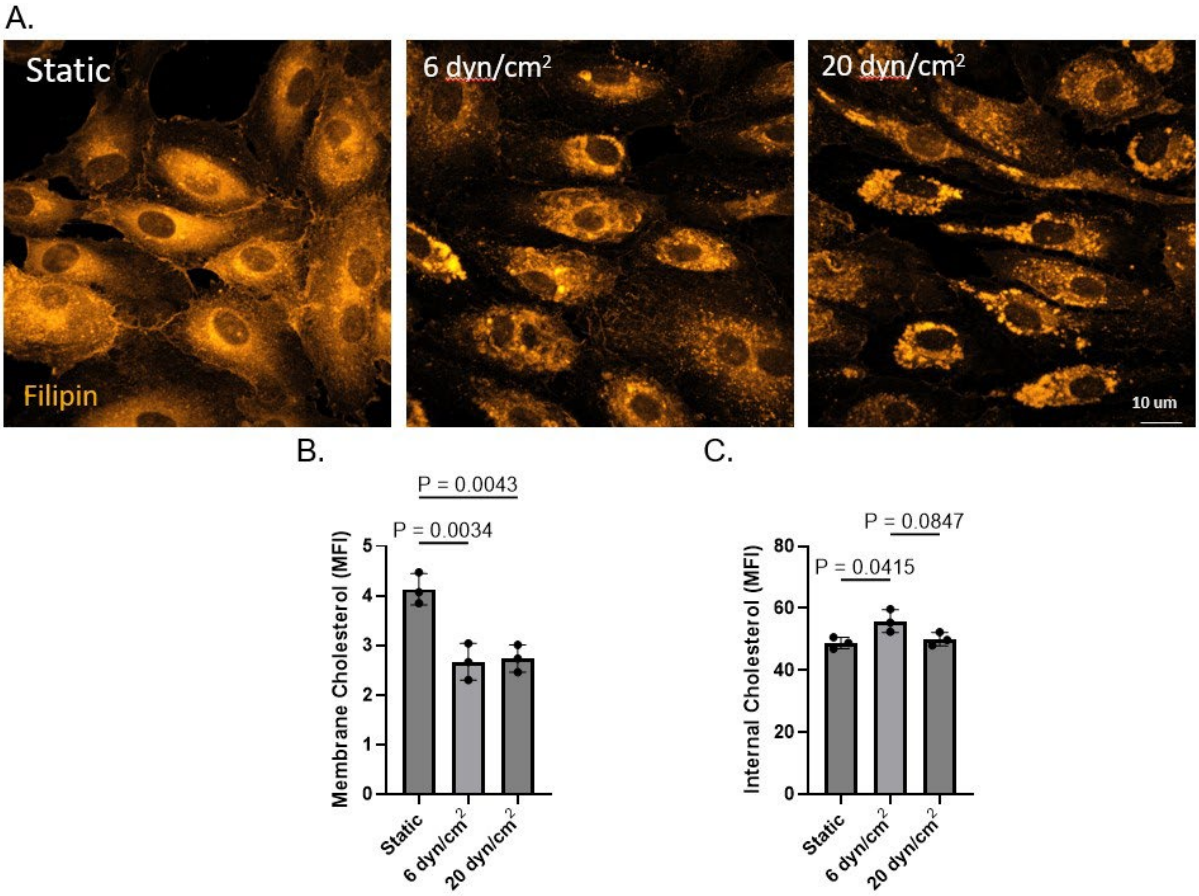

448

449

450

451

452 Fig 3

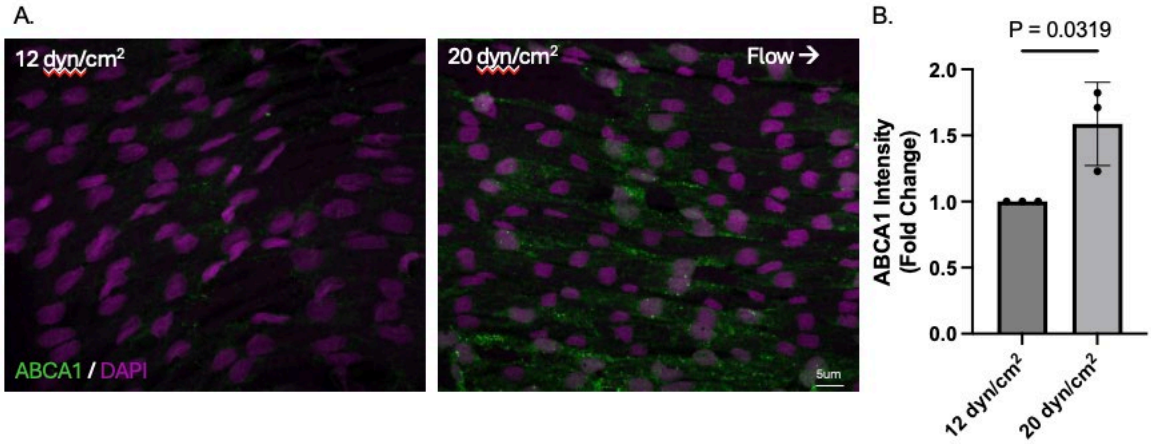

453

454

455

456

457

458

459 Fig 4.

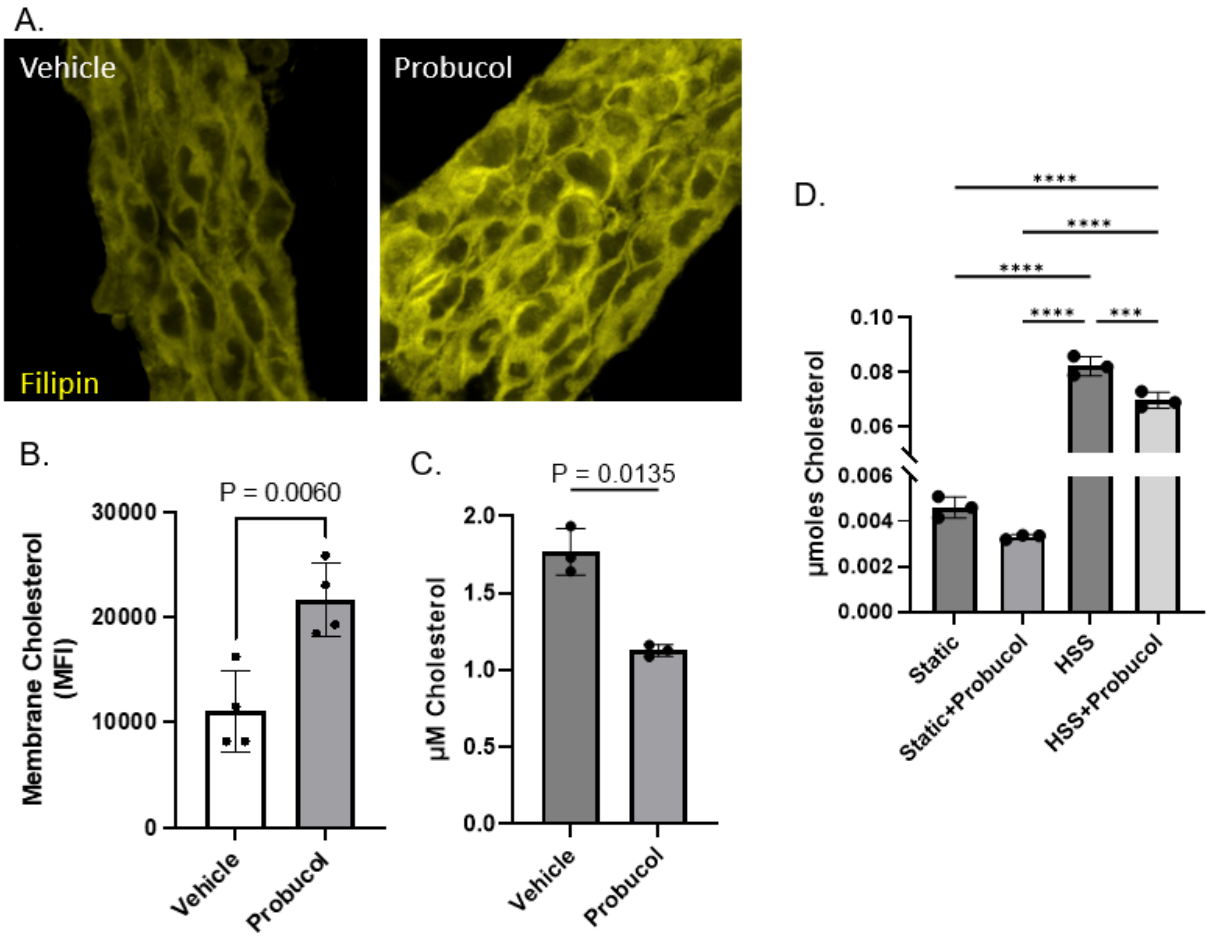

460

461 Fig 5.

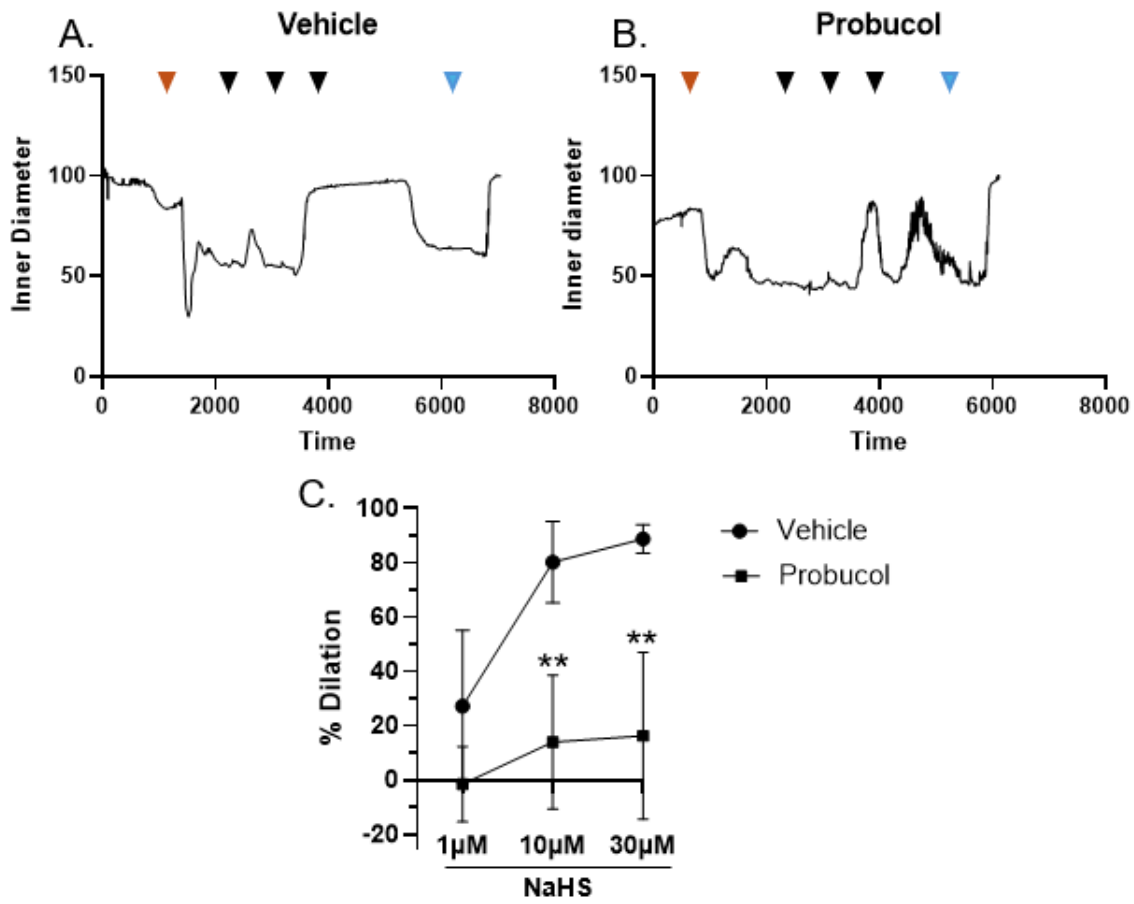

462

463

464

465 Fig 6.

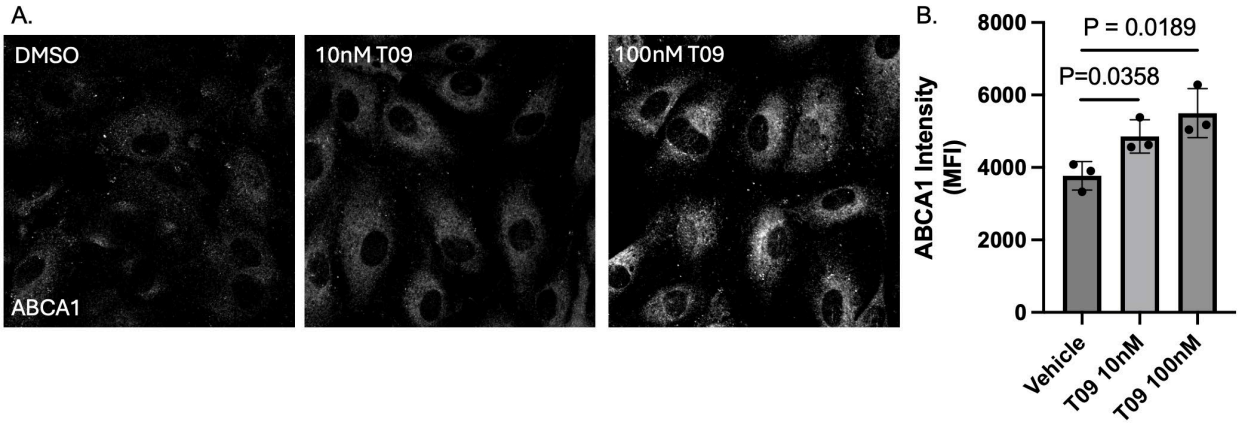
A.
DMSO
10nM T09
100nM T09
ABCA1
B.
8000
6000
4000
2000
0
ABCA1 Intensity (MFI)
P = 0.0189
P=0.0358
Vehicle
T09 10nM
T09 100nM

466

467 Work cited

468 1. Boulanger, C. M. B. Endothelium.
469 https://www.ahajournals.org/doi/epub/10.1161/ATVBAHA.116.306940 (2016)
470 doi:10.1161/ATVBAHA.116.306940.
471 2. Michiels, C. Endothelial cell functions. *Journal of Cellular Physiology* **196**, 430–443
472 (2003).
473 3. *Vascular Effects of Hydrogen Sulfide: Methods and Protocols*. vol. 2007 (Springer
474 New York, New York, NY, 2019).
475 4. Greaney, J. L. *et al.* Impaired Hydrogen Sulfide–Mediated Vasodilation Contributes
476 to Microvascular Endothelial Dysfunction in Hypertensive Adults. *Hypertension* **69**,
477 902–909 (2017).
478 5. Yang, G. *et al.* Hydrogen Sulfide Protects Against Cellular Senescence *via S* -
479 Sulfhydration of Keap1 and Activation of Nrf2. *Antioxidants & Redox Signaling* **18**,
480 1906–1919 (2013).
481 6. Kanagy, N. L., Szabo, C. & Papapetropoulos, A. Vascular biology of hydrogen
482 sulfide. *American Journal of Physiology-Cell Physiology* **312**, C537–C549 (2017).
483 7. Lv, B. *et al.* Hydrogen sulfide and vascular regulation – An update. *J Adv Res* **27**,
484 85–97 (2020).
485 8. Mendiola, P. J., Morin, E. E., Gonzalez Bosc, L. V., Naik, J. S. & Kanagy, N. L. Role
486 of Cholesterol in the Regulation of Hydrogen Sulfide Signaling within the Vascular
487 Endothelium. *Antioxidants (Basel)* **11**, 1680 (2022).

488 9. Das, A., Brown, M. S., Anderson, D. D., Goldstein, J. L. & Radhakrishnan, A. Three
489 pools of plasma membrane cholesterol and their relation to cholesterol homeostasis.
490 *eLife* **3**, e02882 (2014).
491 10. Anderson, J. R. *et al.* Single-cell transcriptomic heterogeneity between conduit and
492 resistance mesenteric arteries in rats. *Physiological Genomics* **55**, 179–193 (2023).
493 11. Vasiliou, V., Vasiliou, K. & Nebert, D. W. Human ATP-binding cassette (ABC)
494 transporter family. *Hum Genomics* **3**, 281–290 (2009).
495 12. Oram, J. F. & Heinecke, J. W. ATP-Binding Cassette Transporter A1: A Cell
496 Cholesterol Exporter That Protects Against Cardiovascular Disease. *Physiological*
497 *Reviews* **85**, 1343–1372 (2005).
498 13. Zhu, M. *et al.* Laminar Shear Stress Regulates Liver X Receptor in Vascular
499 Endothelial Cells. *Arteriosclerosis, Thrombosis, and Vascular Biology* **28**, 527–533
500 (2008).
501 14. Li, Z. *et al.* Cholesterol efflux regulator ABCA1 exerts protective role against high
502 shear stress-induced injury of HBMECs via regulating PI3K/Akt/eNOS signaling.
503 *BMC Neuroscience* **23**, 61 (2022).
504 15. Vion, A.-C. *et al.* Shear Stress Regulates Endothelial Microparticle Release.
505 *Circulation Research* **112**, 1323–1333 (2013).
506 16. Roux, E., Bougaran, P., Dufourcq, P. & Couffinhal, T. Fluid Shear Stress Sensing by
507 the Endothelial Layer. *Frontiers in Physiology* **11**, (2020).
508 17. Lu, D. & Kassab, G. S. Role of shear stress and stretch in vascular mechanobiology.
509 *J. R. Soc. Interface.* **8**, 1379–1385 (2011).

510 18. Davis, M. J., Earley, S., Li, Y.-S. & Chien, S. Vascular mechanotransduction.
511 *Physiological Reviews* **103**, 1247–1421 (2023).
512 19. Naik, J. S., Osmond, J. M., Walker, B. R. & Kanagy, N. L. Hydrogen sulfide-induced
513 vasodilation mediated by endothelial TRPV4 channels. *Am J Physiol Heart Circ*
514 *Physiol* **311**, H1437–H1444 (2016).
515 20. Rasband, W.S. (1997-2015) ImageJ. National Institutes of Health, Bethesda,
516 Maryland, USA. - References - Scientific Research Publishing.
517 https://www.scirp.org/reference/referencespapers?referenceid=1690059.
518 21. Wenceslau, C. F. *et al.* Guidelines for the measurement of vascular function and
519 structure in isolated arteries and veins. *American Journal of Physiology-Heart and*
520 *Circulatory Physiology* **321**, H77–H111 (2021).
521 22. Garcia, S. M., Naik, J. S., Resta, T. C. & Jernigan, N. L. Acid-sensing ion channel 1a
522 activates IKCa/SKCa channels and contributes to endothelium-dependent dilation.
523 *Journal of General Physiology* **155**, e202213173 (2022).
524 23. Morin, E. E., Salbato, S., Walker, B. R. & Naik, J. S. Endothelial cell membrane
525 cholesterol content regulates the contribution of TRPV4 channels in ACh-induced
526 vasodilation in rat gracilis arteries. *Microcirculation* **29**, e12774 (2022).
527 24. Anderson, J. R. *et al.* Single-cell transcriptomic heterogeneity between conduit and
528 resistance mesenteric arteries in rats. *Physiol Genomics* **55**, 179–193 (2023).
529 25. Drożdż, D., Drożdż, M. & Wójcik, M. Endothelial dysfunction as a factor leading to
530 arterial hypertension. *Pediatr Nephrol* **38**, 2973–2985 (2023).
531 26. Beverley, K. M. & Levitan, I. Cholesterol regulation of mechanosensitive ion
532 channels. *Front. Cell Dev. Biol.* **12**, (2024).

533 27. Liu, K. *et al.* Inhibiting NF- B increases cholesterol efflux from THP-1 derived- foam
534 cells treated with AngII via up-regulating the expression of ATP-binding cassette
535 transporter A. *Journal of Nanjing Medical University* (2008).
536 28. Ferreira, V. *et al.* Macrophage-specific inhibition of NF-κB activation reduces foam-
537 cell formation. *Atherosclerosis* **192**, 283–290 (2007).
538 29. Krimbou, L. *et al.* Molecular interactions between apoE and ABCA1. *Journal of Lipid*
539 *Research* **45**, 839–848 (2004).
540 30. Getz, G. S. & Reardon, C. A. Apoprotein E and Reverse Cholesterol Transport. *Int J*
541 *Mol Sci* **19**, 3479 (2018).
542 31. Mao, H. *et al.* Endothelial LRP1 regulates metabolic responses by acting as a co-
543 activator of PPARγ. *Nat Commun* **8**, 14960 (2017).
544 32. Chawla, A. *et al.* A PPARγ-LXR-ABCA1 Pathway in Macrophages Is Involved in
545 Cholesterol Efflux and Atherogenesis. *Molecular Cell* **7**, 161–171 (2001).
546 33. Ghanbari-Niaki, A. *et al.* Heart ABCA1 and PPAR- α Genes Expression Responses
547 in Male Rats: Effects of High Intensity Treadmill Running Training and Aqueous
548 Extraction of Black Crataegus-Pentaegyna. *Research in Cardiovascular Medicine* **2**,
549 153 (2013).
550 34. Oram, J. F., Wolfbauer, G., Vaughan, A. M., Tang, C. & Albers, J. J. Phospholipid
551 Transfer Protein Interacts with and Stabilizes ATP-binding Cassette Transporter A1
552 and Enhances Cholesterol Efflux from Cells *. *Journal of Biological Chemistry* **278**,
553 52379–52385 (2003).

554 35. Kumari, S. *et al.* Influence of membrane cholesterol in the molecular evolution and
555 functional regulation of TRPV4. *Biochemical and Biophysical Research*
556 *Communications* **456**, 312–319 (2015).
557 36. Singh, A. K. *et al.* Multiple Cholesterol Recognition/Interaction Amino Acid
558 Consensus (CRAC) Motifs in Cytosolic C Tail of Slo1 Subunit Determine Cholesterol
559 Sensitivity of Ca2+- and Voltage-gated K+ (BK) Channels. *J Biol Chem* **287**, 20509–
560 20521 (2012).
561 37. Wang, X.-L. *et al.* Caveolae Targeting and Regulation of Large Conductance Ca2+-
562 activated K+ Channels in Vascular Endothelial Cells. *Journal of Biological Chemistry*
563 **280**, 11656–11664 (2005).
564 38. Mendiola, P. J., Morin, E. E., Gonzalez Bosc, L. V., Naik, J. S. & Kanagy, N. L. Role
565 of Cholesterol in the Regulation of Hydrogen Sulfide Signaling within the Vascular
566 Endothelium. *Antioxidants (Basel)* **11**, 1680 (2022).
567 39. Sriram, K., Laughlin, J. G., Rangamani, P. & Tartakovsky, D. M. Shear-Induced Nitric
568 Oxide Production by Endothelial Cells. *Biophys J* **111**, 208–221 (2016).
569 40. Wojciak-Stothard, B. & Ridley, A. J. Shear stress–induced endothelial cell
570 polarization is mediated by Rho and Rac but not Cdc42 or PI 3-kinases. *J Cell Biol*
571 **161**, 429–439 (2003).
572 41. Zakkar, M., Angelini, G. D. & Emanueli, C. Regulation of Vascular Endothelium
573 Inflammatory Signalling by Shear Stress. *http://www.eurekaselect.com*.
574 42. Meng, Q. *et al.* Laminar shear stress inhibits inflammation by activating autophagy in
575 human aortic endothelial cells through HMGB1 nuclear translocation. *Commun Biol*
576 **5**, 1–13 (2022).

577 43. Seebach, J. *et al.* Endothelial Barrier Function under Laminar Fluid Shear Stress.
578 *Lab Invest* **80**, 1819–1831 (2000).
579 44. Neufeld, E. B. *et al.* Cellular Localization and Trafficking of the Human ABCA1
580 Transporter * 210. *Journal of Biological Chemistry* **276**, 27584–27590 (2001).
581 45. Zeng, L. *et al.* Sterol-responsive element-binding protein (SREBP) 2 down-regulates
582 ATP-binding cassette transporter A1 in vascular endothelial cells: a novel role of
583 SREBP in regulating cholesterol metabolism. *J Biol Chem* **279**, 48801–48807
584 (2004).
585 46. Arakawa, R. & Yokoyama, S. Helical Apolipoproteins Stabilize ATP-binding Cassette
586 Transporter A1 by Protecting It from Thiol Protease-mediated Degradation *. *Journal*
587 *of Biological Chemistry* **277**, 22426–22429 (2002).
588 47. Azuma, Y. *et al.* Retroendocytosis pathway of ABCA1/apoA-I contributes to HDL
589 formation. *Genes to Cells* **14**, 191–204 (2009).
590